Magazine of Concrete Research

Structural behaviour of reinforced concrete beams containing crumb rubber and steel fibres
Ismail, Hassan and Hussein

Magazine of Concrete Research
http://dx.doi.org/10.1680/jmacr.16.00525
**Paper 1600525**
Received 03/12/2016; revised 13/03/2017; accepted 13/03/2017
**Keywords:** composite materials/fibre-reinforced concrete/shear


ice
Institution of Civil Engineers
publishing

# Structural behaviour of reinforced concrete beams containing crumb rubber and steel fibres

**Mohamed K. Ismail**
Faculty of Engineering and Applied Science, Memorial University of Newfoundland, St. John's, NL, Canada

**Assem A. A. Hassan**
Faculty of Engineering and Applied Science, Memorial University of Newfoundland, St. John's, NL, Canada (corresponding author: ahassan@mun.ca)

**Amgad A. Hussein**
Faculty of Engineering and Applied Science, Memorial University of Newfoundland, St. John's, NL, Canada

**This paper presents experimental work to investigate the strength and cracking characteristics of optimised self-consolidating and vibrated rubberised concrete mixtures with/without steel fibres (SFs) using large-scale reinforced concrete beams. The test beams were cast with varying percentages of crumb rubber (CR) (0 to 35%), SF volume fractions (0, 0·35 and 1%) and SF lengths (35 and 60 mm). The performance of some design codes and published empirical equations was evaluated in predicting the shear capacity and first cracking moment of the tested beams. The results showed that the inclusion of SFs could alleviate the reduction in the shear capacity and first cracking moment that resulted from the addition of CR. In addition, combining CR and SFs contributed to developing sustainable concrete beams with high deformability, reduced self-weight and improved shear capacity. The composite effect of CR and SFs also helped to narrow the developed cracks and change the failure mode from brittle shear failure into ductile flexural failure, particularly for the SF volume of 1% (35 mm length). Comparisons of the predicted and experimental results indicate that most of the proposed equations can satisfactorily estimate the shear strength, but overestimate the first cracking moment.**

## Notation

| | |
|---|---|
| $b$ | width of beam (mm) |
| $d$ | effective depth of beam (mm) |
| $f_{ck}$ | characteristic compressive cylinder strength of concrete at 28 d |
| $f_{ctm}$ | mean value of axial tensile strength of concrete |
| $f'_c$ | 28 d compressive strength |
| $f'_{cf}$ | characteristic flexural tensile strength of concrete |
| $h$ | height of cross-section of beam |
| $I_g$ | second moment of area of gross section |
| $I_u$ | second moment of area of uncracked transformed section |
| $M_{cr}^{exp}$ | experimental first cracking moment |
| $M_{cr}^{pred}$ | predicted first cracking moment |
| $V_{exp}$ | experimental shear capacity |
| $V_{pred}$ | predicted shear capacity |
| $V_u$ | ultimate shear load |
| $v_{nz}$ | normalised shear strength ($v_{nz}$) |
| $x_u$ | distance from neutral axis of the section to the extreme top fibre |
| $y_t$ | distance from the centroidal axis of the gross section to the extreme tension fibre |
| $Z$ | section modulus ($= I/y$) |

## Introduction

Reutilisation of scrap rubber in concrete is being increasingly adopted as a possible safe technique to exploit huge volumes of this problematic waste material and produce a new type of sustainable concrete. In the last two decades, extensive research has been conducted to evaluate the impact of using rubber on the properties of concrete. From the data available in the literature, adding rubber to small-scale samples (i.e. cubes, cylinders and prisms) appeared to boost their impact resistance, damping properties, energy dissipation and ductility, and also reduced the self-weight of the concrete (Ismail and Hassan, 2016a; Najim and Hall, 2012; Zheng *et al.*, 2008). However, all the studies confirmed that the compressive and tensile strengths of these concrete composites were negatively affected by the inclusion of rubber. This was related to (*a*) the poor strength of the rubber–mortar interface and (*b*) the significant difference between the modulus of elasticity of rubber particles and that of cement mortar (Najim and Hall, 2010).

Some studies involved the use of rubber in large-scale structural members. For example, Ganesan *et al.* (2013) investigated the influence of shredded rubber on the performance of self-consolidating rubberised concrete (SCRC) beam–column joints under monotonic and cyclic loading. They reported that the inclusion of rubber increased the energy absorption capacity, crack resistance and ductility of the concrete. Youssf *et al.* (2015) observed similar effects when rubber was added; the hysteretic damping ratio and energy dissipation of concrete columns subjected to cyclic loading were found to be improved when crumb rubber (CR) was added, but the ultimate lateral load slightly decreased. Other researchers (Ismail and Hassan, 2015a; Najim and Hall, 2014) have reported that reinforced beams made with SCRC and vibrated rubberised concrete (VRC) showed lower flexural capacity and stiffness compared with beams made without rubber, while the deformation capacity and energy absorption increased with an increase in rubber content. Sadek and El-Attar (2014) reported that the inclusion of rubber in masonry walls increased their toughness, deformation capacity and capability to withstand post-failure loads. None of the studies conducted have reported on the shear behaviour of rubberised concrete, although cracking behaviour and the cracking mechanism, which affect the shear behaviour of concrete (Taylor, 1974), may be influenced by the addition of CR.

Reinforcing rubberised concrete with steel fibres (SFs) can effectively contribute to the development of composites with higher tensile strength, toughness and impact strength (Abadel *et al.*, 2015; Altun and Aktas, 2013; Ismail and Hassan, 2016a; Khaloo *et al.*, 2014; Olivito and Zuccarello, 2010). SFs also play a significant role in transferring stress along cracked sections, which in turn provides a residual strength to concrete, and hence increases the shear capacity of concrete beams, as reported by other researchers (Ding *et al.*, 2011, 2012; Tahenni *et al.*, 2016). In addition, the fibres' bridging mechanism can help to restrain the development of cracks and limit crack openings (Ganesan *et al.*, 2014; Lee *et al.*, 2016).

The beneficial effects that come from using SFs in rubberised concrete can be maximised when self-consolidating concrete (SCC) is used. Coupling rubber and SFs in SCC can offer a novel type of sustainable concrete that enjoys the desirable properties of SCC in the fresh state and also has higher ductility, toughness, impact resistance and reduced self-weight in the hardened state. However, optimising the fresh properties of SCC incorporating rubber and SFs is a big challenge. As shown in past studies, the addition of rubber has negative effects on the flowability, passing ability and stability of SCC mixtures (Güneyisi, 2010; Ismail and Hassan, 2015b; Topçu and Bilir, 2009). Similarly, SCC with the addition of SFs appears to suffer from high interference between the SFs and coarse aggregates, which leads to a significant decrease in the flowability and passing ability of mixtures (Ding *et al.*, 2008; Iqbal *et al.*, 2015).

The universal design codes provide several models to estimate the shear strength of concrete. Some of these models were proposed based purely on empirical procedures, such as ACI 318 (ACI, 2008) and Eurocode 2 (EC2) (BSI, 2005), while other models were derived from fundamentals presented in the modified compression field theory, such as the Aashto LRFD code (Aashto, 2007). With much easier assumptions, the shear design model of CSA A23.3 (CSA, 2004) was developed based on simplified modified compression field theory. However, these code models do not include the effect of SFs, which has encouraged many investigators to adapt the code equations or propose new empirical models in attempts to estimate the contribution of SFs to the shear capacity of reinforced concrete beams. For example, Ashour *et al.* (1992) and Khuntia *et al.* (1999) adjusted the ACI 318 equation (ACI, 2008) to account for the contribution of SFs and incorporated new terms such as the SF fraction volume, aspect ratio and geometry. On the other hand, other researchers have developed shear models based on their own experiments and results available in the literature. Sharma (1986) proposed a simple model derived from experiments conducted in his investigation and data obtained from Baston *et al.* (1972). Although this model was validated by a significant number of studies, it lacks some factors that are known to greatly affect the shear strength, such as fibre volume, fibre aspect ratio and flexural reinforcement ratio. These factors, in addition to others such as the effect of the fibres' bond stresses, were covered in a model proposed by Narayanan and Darwish (1987). Imam *et al.* (1994) modified the equation proposed by Bazant and Sun (1987), which was suggested to predict the shear strength of conventional concrete beams in order to consider the contribution of fibres. The modified model appeared to be different from most of the other available models in that the effect of maximum aggregate size on the shear strength of concrete beams was considered. An equation proposed by Zsutty (1971) was adapted by Kwak *et al.* (2002) to account for the effect of tensile strength on arching action, with a new term added to consider the effect of fibres on the shear strength of beams.

Despite active research aiming to evaluate the performance of rubberised concrete with/without SFs, no study has covered the effect of CR with/without SFs on the shear behaviour of large-scale beams, especially when SCC is used. In addition, evaluating the capability of the proposed equations to predict the performance of rubberised concrete beams with/without SFs in terms of shear capacity and first cracking moment is lacking, because this type of concrete is a novel material. The study reported here was thus carried out to highlight the effect of CR with/without SFs on the shear behaviour and cracking characteristics of large-scale reinforced concrete beams with no stirrups. The performance of some code design equations and different proposed models on the shear behaviour and cracking moment was also evaluated. The tested beams were fabricated with varying percentages of CR (0 to 35%), different SF volume fractions (0, 0·35 and 1%) and different SF lengths (35 and 60 mm).

## Research significance

Developing structural concrete with low-density waste rubber aggregate and reinforced with SFs can contribute to the development of sustainable concrete with a high-impact resistance and deformability and reduced self-weight. This research was conducted to evaluate the influence of CR with/without SFs on the shear capacity and cracking characteristics of reinforced concrete beams made with SCC and VRC. The research also compared the experimental results with the performance of the code design equations commonly used to predict the shear strength and cracking moment of concrete beams. A review of the literature indicated that no study has covered the shear behaviour and cracking characteristics of large-scale rubberised concrete beams with/without SFs, especially when made with SCC. This investigation is therefore intended to help further the understanding of the shear behaviour and cracking characteristics of SCRC, VRC, steel-fibre-reinforced SCRC (SFSCRC) and steel-fibre-reinforced VRC (SFVRC) in order to extend the possible applications of CR in the construction industry.

## Experimental programme

### Material properties

Type GU Canadian Portland cement, similar to type 1 ASTM C150 cement (ASTM, 2012b), metakaolin (MK) conforming to ASTM C618 class N (ASTM, 2012a) and fly ash similar to ASTM C618 type F (ASTM, 2012a) were used as binders for all the developed mixtures. Natural crushed stone of 10 mm maximum size and natural sand were used for the coarse and fine aggregates, respectively, with a specific gravity of 2·6 and water absorption of 1%. In this study, the fine aggregate was partially replaced by CR aggregate, which had a maximum size of 4·75 mm, a specific gravity of 0·95 and negligible water absorption. Two types of SFs with hooked ends (Dramix 3D) were used: the first type were 35 mm long and 0·55 mm in diameter with an aspect ratio of 65; the second type were 60 mm long and 0·9 mm in diameter, again with an aspect ratio of 65. Each type of SF had a tensile strength of 1050 MPa, Young's modulus of 210 GPa and density of 7·85 kg/m$^3$. A polycarboxylate-based high-range water-reducing admixture (HRWRA) similar to ASTM C494 type F (ASTM, 2013), with a specific gravity of 1·2, volatile weight of 62% and pH of 9·5, was used to achieve the required workability of the test mixtures. The steel bars used in the constructed beams had an average yield stress of 417 MPa.

### Concrete mixtures

In total, 12 concrete mixtures were developed to cast 12 reinforced concrete beams. These mixtures were derived from a comprehensive investigation conducted by the authors on optimising the fresh and mechanical properties of SCRC, VRC, SFSCRC and SFVRC mixtures. The results of this study indicated that a total binder content of at least 550 kg/m$^3$ with a minimum water/binder (w/b) ratio of 0·4 should be used to obtain acceptable slump flow and no visual sign of segregation. Replacement of cement by 30% fly ash and 20% MK was found to be an optimum choice for adjusting the mixtures' viscosity, in which a good particle suspension was achieved with reasonable flowability. In addition, 20% MK contributed to the development of mixtures with enhanced mechanical properties, suitable for structural applications (Ismail and Hassan, 2016b). The coarse to fine aggregate ratio was kept constant at 0·7 for all the tested mixtures.

The chosen mixtures were used in two stages of work and details of all the mixtures are given in Table 1.

The first stage included (*a*) four SCRC mixtures with CR percentage varying from 0 to 25% (mixtures 1–4), developed to evaluate the effect of CR on the shear behaviour and cracking of SCRC beams, and (*b*) two SFSCRC mixtures with 0·35% SFs (35 mm) having 5% and 15% CR (mixtures 5 and 6), developed to investigate the effect of combining CR and SFs on the shear behaviour and cracking of SCRC beams. Mixtures 1–6 were developed with the maximum percentage of CR (with/without SFs) that could be used in SCC mixtures to successfully fulfil the self-compactability criteria, as per the European guidelines for self-compacting concrete (Efnarc, 2005). Further increasing the percentage of CR and/or SFs in these mixtures (1–6) led to a significant reduction in the passing ability below the acceptable limits ($H_2/H_1$ of L-box $\geq 0{\cdot}75$) (Efnarc, 2005). Similarly, in this stage, fibres longer than 35 mm could not be used because high blockage occurred in the L-box, which made it difficult for mixtures to pass through the rebars.

For these reasons, stage 2 was constructed to evaluate the effect of using higher percentages of CR (with/without SFs) and longer fibres on the strength and cracking of the tested beam. Unlike SCC mixtures, vibrated concrete does not require high flowability and passing ability. Therefore, it was possible to combine a maximum of 35% CR and 1% SF in the VRC mixtures in stage 2. Different SF lengths (35 and 60 mm) could also be tested in this stage. The second stage thus included (*a*) two VRC mixtures with 25% and 35% CR (mixtures 7 and 8), (*b*) two SFVRC mixtures with 35% CR having 0·35% and 1% SFs (35 mm length) and (*c*) two SFVRC mixtures with 35% CR having 0·35% and 1% SFs (60 mm length). The maximum percentage of CR (35%) in the second stage was chosen based on the 28 d compressive strength: a further increase in CR content resulted in a significant reduction in compressive strength. However, a VRC mixture with 25% CR was included in this study to investigate the influence of concrete type (i.e. SCRC compared to VRC).

The tested beams/mixtures were designated by concrete type (whether SCC or vibrated concrete (VC)), percentage of CR, and the volume and size of SFs used (see Table 1). For example, a beam/mixture using SCC, 15% CR and 0·35%

Table 1. Mixture designs for tested beams

| Beam | Mixture | Cement: kg/m$^3$ | MK: kg/m$^3$ | Fly ash: kg/m$^3$ | CA: kg/m$^3$ | FA: kg/m$^3$ | CR: kg/m$^3$ | SF: kg/m$^3$ | Density: kg/m$^3$ |
|---|---|---|---|---|---|---|---|---|---|
| SCRC/SFSCRC mixtures | | | | | | | | | |
| B1 | SCC-0CR | 275 | 110 | 165 | 620·3 | 886·1 | 0·0 | — | 2246 |
| B2 | SCC-5CR | 275 | 110 | 165 | 620·3 | 841·8 | 16·2 | — | 2207 |
| B3 | SCC-15CR | 275 | 110 | 165 | 620·3 | 753·2 | 48·6 | — | 2128 |
| B4 | SCC-25CR | 275 | 110 | 165 | 620·3 | 664·6 | 80·9 | — | 2041 |
| B5 | SCC-5CR-0·35SF | 275 | 110 | 165 | 616·5 | 836·7 | 16·1 | 27·48 | 2217 |
| B6 | SCC-15CR-0·35SF | 275 | 110 | 165 | 616·5 | 748·6 | 48·3 | 27·48 | 2138 |
| VRC/SFVRC mixtures | | | | | | | | | |
| B7 | VC-25CR | 275 | 110 | 165 | 620·3 | 664·6 | 80·9 | — | 2048 |
| B8 | VC-35CR | 275 | 110 | 165 | 620·3 | 576·0 | 113·3 | — | 2014 |
| B9 | VC-35CR-0·35SF | 275 | 110 | 165 | 616·5 | 572·5 | 112·6 | 27·48 | 2040 |
| B10 | VC-35CR-1SF | 275 | 110 | 165 | 609·6 | 566·0 | 111·4 | 78·50 | 2073 |
| B11 | VC-35CR-0·35LSF | 275 | 110 | 165 | 616·5 | 572·5 | 112·6 | 27·48 | 2040 |
| B12 | VC-35CR-1LSF | 275 | 110 | 165 | 609·6 | 566·0 | 111·4 | 78·50 | 2073 |

Note: All mixtures had a 0·4 w/b ratio and a 0·7 coarse/fine aggregate ratio
CA, coarse aggregate; FA, fine aggregate; SF, steel fibre; LSF, long steel fibre

Table 2. Fresh and mechanical properties of tested mixtures

| Beam | Mixture | $T_{50}$: s | V-funnel $T_0$: s | L-box ratio: $H_2/H_1$ | SR: % | Slump: mm | Air: % | HRWRA: l/m$^3$ | $f_c'$: MPa | STS: MPa |
|---|---|---|---|---|---|---|---|---|---|---|
| SCRC/SFSCRC | | | | | | | | | | |
| B1 | SCC-0CR | 2 | 7·0 | 0·91 | 2·1 | — | 1·5 | 3·43 | 65·6 | 4·0 |
| B2 | SCC-5CR | 2·4 | 8·5 | 0·88 | 2·7 | — | 2·0 | 3·43 | 58·4 | 3·7 |
| B3 | SCC-15CR | 3 | 10·6 | 0·82 | 5·8 | — | 3·1 | 3·75 | 48·4 | 3·3 |
| B4 | SCC-25CR | 3·4 | 14·3 | 0·77 | 8·3 | — | 4·6 | 3·75 | 38·4 | 2·8 |
| B5 | SCC-5CR-0·35SF | 2·6 | 9·8 | 0·8 | 2·9 | — | 2·4 | 4·63 | 59·2 | 4·4 |
| B6 | SCC-15CR-0·35SF | 3·3 | 12·1 | 0·75 | 6·0 | — | 3·5 | 4·63 | 49·5 | 3·9 |
| VRC/SFVRC | | | | | | | | | | |
| B7 | VC-25CR | | — | | | 180 | 3·0 | 3·18 | 40·3 | 2·8 |
| B8 | VC-35CR | | — | | | 145 | 3·3 | 3·18 | 29·7 | 2·5 |
| B9 | VC-35CR-0·35SF | | — | | | 185 | 3·0 | 3·64 | 31·1 | 3·2 |
| B10 | VC-35CR-1SF | | — | | | 85 | 3·1 | 3·64 | 32·4 | 4·4 |
| B11 | VC-35CR-0·35LSF | | — | | | 170 | 3·2 | 3·64 | 30·7 | 3·4 |
| B12 | VC-35CR-1LSF | | — | | | 80 | 3·4 | 3·64 | 31·5 | 4·7 |

SR, segregation resistance

short SFs (35 mm length) is labelled as SCC-15CR-0·35SF and a beam/mixture using VC, 35% CR and 1% long SFs (60 mm length) is labelled as VC-35CR-1LSF.

The behaviour of the SCC/SCRC/SFSCRC mixtures in the fresh state was evaluated using slump flow, V-funnel, L-box and sieve segregation tests according to Efnarc (2005). A slump test was used to assess the workability of VRC/SFVRC according to ASTM C143 (ASTM, 2015). The percentage of air content in all the developed mixtures was measured in the fresh state according to ASTM C231 (ASTM, 2014). Tests for 28 d compressive strength and splitting tensile strength (STS) were conducted using 100 mm diameter × 200 mm height concrete cylinders according to ASTM C39 (ASTM, 2011a) and C496 (ASTM, 2011b), respectively. The compressive strength and STS tests were implemented after the sample had been exposed to a curing condition similar to that used for the test beams. The results of the fresh properties, 28 d compressive strength and STS of the tested mixtures are given in Table 2.

## Shear test setup, instrumentation and loading procedure

All beams were cast without shear reinforcement and tested under a four-point symmetrical vertical loading condition until shear failure (Figure 1). A single load was applied through a hydraulic actuator (with a capacity of 500 kN) and then distributed into two-point loads acting on the top surface of the beam. The shear span-to-depth ratio was kept constant at

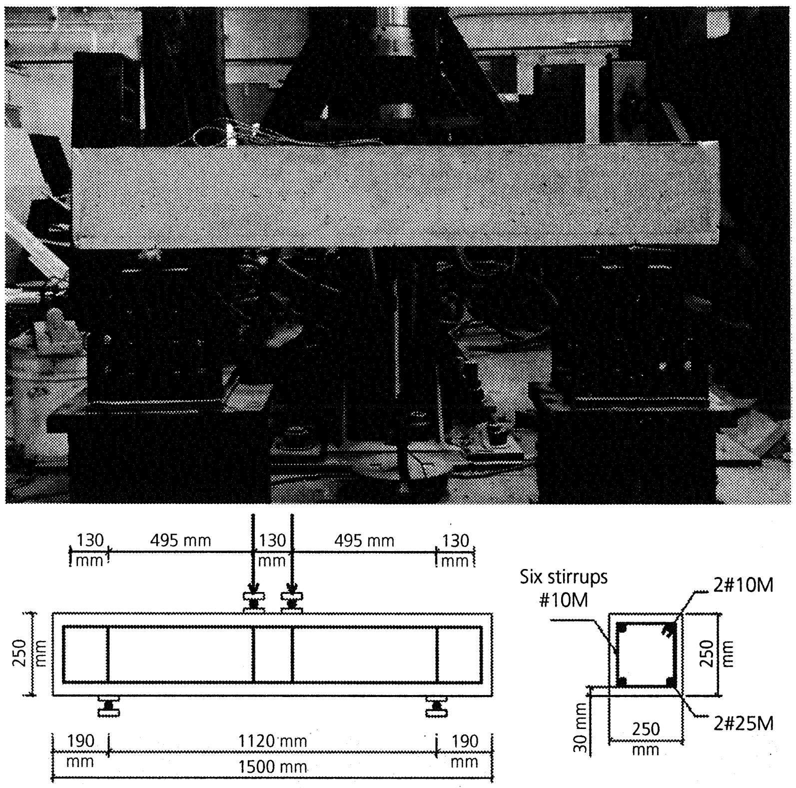


Figure 1. Typical test setup, dimensions and reinforcement of tested beams

2·5 for all tested beams. The mid-span deflection of the tested beams was measured using a linear variable differential transformer. The beams were loaded gradually, with a constant loading rate up to the first cracking load and the failure load. After each stage of loading, the cracks were marked and a crack detection microscope (60× magnification with 0·02 mm least count) was used to accurately measure their widths. The overall behaviour of the beams, including the cracking characteristics (patterns, widths, heights and angles) and failure modes, was observed and sketched for all beams (see Figure 2). The results obtained from the shear testing of the 12 beams are presented in Table 3.

## Discussion of test results

### Experimental load–deflection curve

Figure 3 shows the load–mid-span deflection curves of the tested beams. Figure 3(a) shows that the beams made with CR (B2, B3 and B4) appeared to behave similarly to the beam B1 without CR. In general, up to the first cracking load, all the tested beams showed elastic behaviour where the deflection was linearly proportional to the applied load. Beyond the first crack, the curves were almost linear but with a slightly lower slope as the beams' stiffness decreased due to the formation of macrocracks. With a further increase in applied load, the curves deviated from linearity and a higher rate of deflection was exhibited until the occurrence of failure. From Figure 3(a), it can also be seen that increasing the percentage of CR from 0 to 25% (B1 to B4) appeared to increase the deformability of the SCRC beams at a given load, which indicates a reduction in beam stiffness with increasing CR content. Similar behaviour was observed in the VRC beams when the percentage of CR was increased from 25 to 35% (B7 to B8), as shown in Figure 3(b). Such a decrease in stiffness was due to replacing the conventional sand with flexible rubber particles, which in turn decreased the overall stiffness of the tested SCRC and VRC beams. Comparing the load–deflection curve of the SCRC beam (B4) with its counterpart VRC beam (B7) in Figure 3(b) reveals that, up to almost 70% of the failure load, both beams showed comparable behaviour but beyond this load level the SCRC beam (B4) experienced slightly higher deformation than the VRC beam (B7).

Assessing the effect of including 0·35% SFs, Figures 3(c) and 3(d) show that the SFSCRC (B5 and B6) and SFVRC (B9) beams with 0·35% SFs presented a slightly increased stiffness

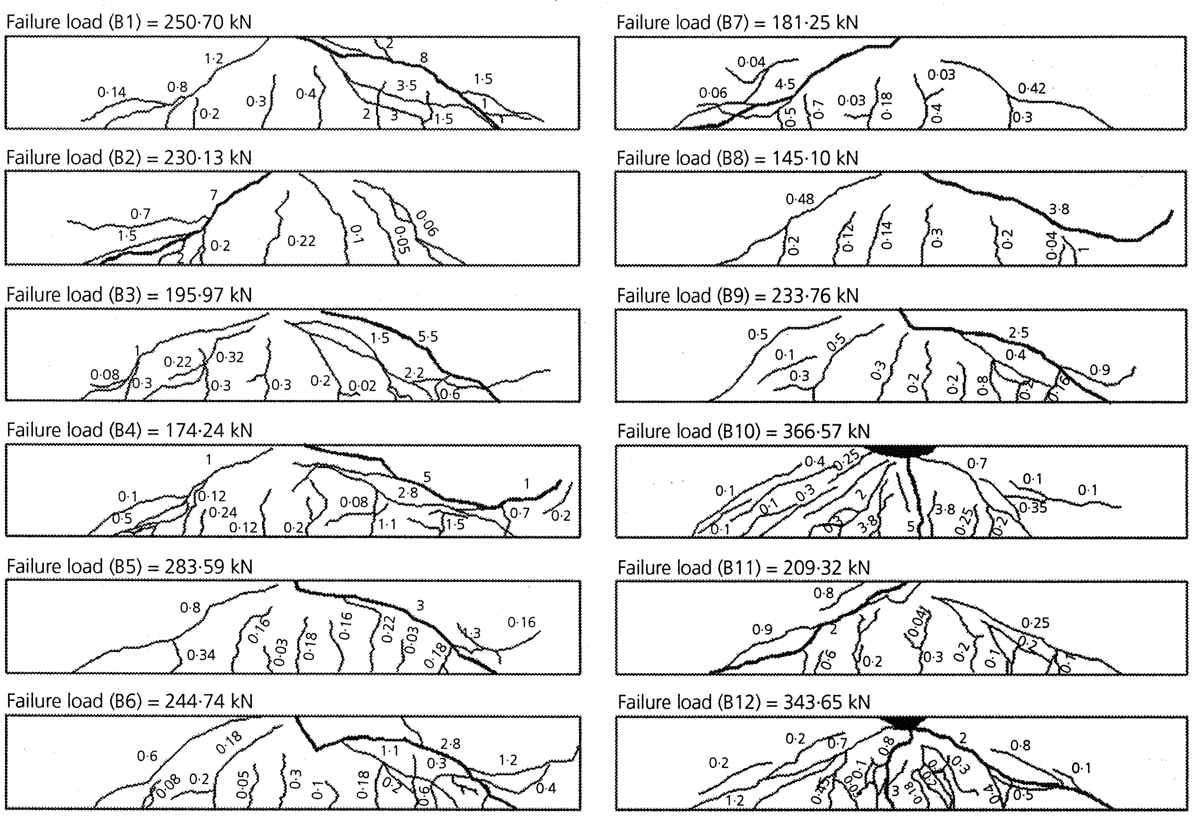


**Figure 2.** Crack patterns of tested beams at failure (crack widths in mm)

**Table 3.** Results of beam shear tests

| Beam | Experimental first cracking moment: kN.m | Ultimate shear load, $V_u$: kN | Normalised shear strength, $v_{n2}$ | Failure mode | At failure: Number of cracks | At failure: Maximum crack width: mm | At failure: Failure angle: degrees |
|---|---|---|---|---|---|---|---|
| SCRC/SFSCRC | | | | | | | |
| B1 | 10·9 | 125·35 | 0·31 | Shear | 9 | 8 | 37 |
| B2 | 9·7 | 115·07 | 0·30 | Shear | 10 | 7 | 28 |
| B3 | 8·0 | 97·99 | 0·29 | Shear | 11 | 5·5 | 33 |
| B4 | 6·5 | 87·12 | 0·28 | Shear | 11 | 5 | 30 |
| B5 | 11·0 | 141·80 | 0·37 | Shear | 10 | 3 | 31 |
| B6 | 9·1 | 122·37 | 0·35 | Shear | 12 | 2·8 | 32 |
| VRC/SFVRC | | | | | | | |
| B7 | 6·7 | 90·63 | 0·29 | Shear | 8 | 4·5 | 27 |
| B8 | 5·3 | 72·55 | 0·27 | Shear | 9 | 3·8 | 21 |
| B9 | 6·2 | 116·88 | 0·42 | Shear | 9 | 2·5 | 28 |
| B10 | 7·7 | 183·29 | 0·65 | Flexure | 12 | 5 | — |
| B11 | 5·8 | 104·66 | 0·38 | Shear | 11 | 2 | 26 |
| B12 | 7·2 | 171·83 | 0·62 | Flexure-shear | 13 | 3 | — |

and maximum deflection at ultimate load compared with their counterpart beams without SFs (B2 and B3, and B8, respectively). However, adding a higher volume of fibres (1%) increased the beams' stiffness and allowed the beams to sustain higher ultimate load accompanied with larger corresponding deflections (B10 and B12 compared with B8). This indicates a

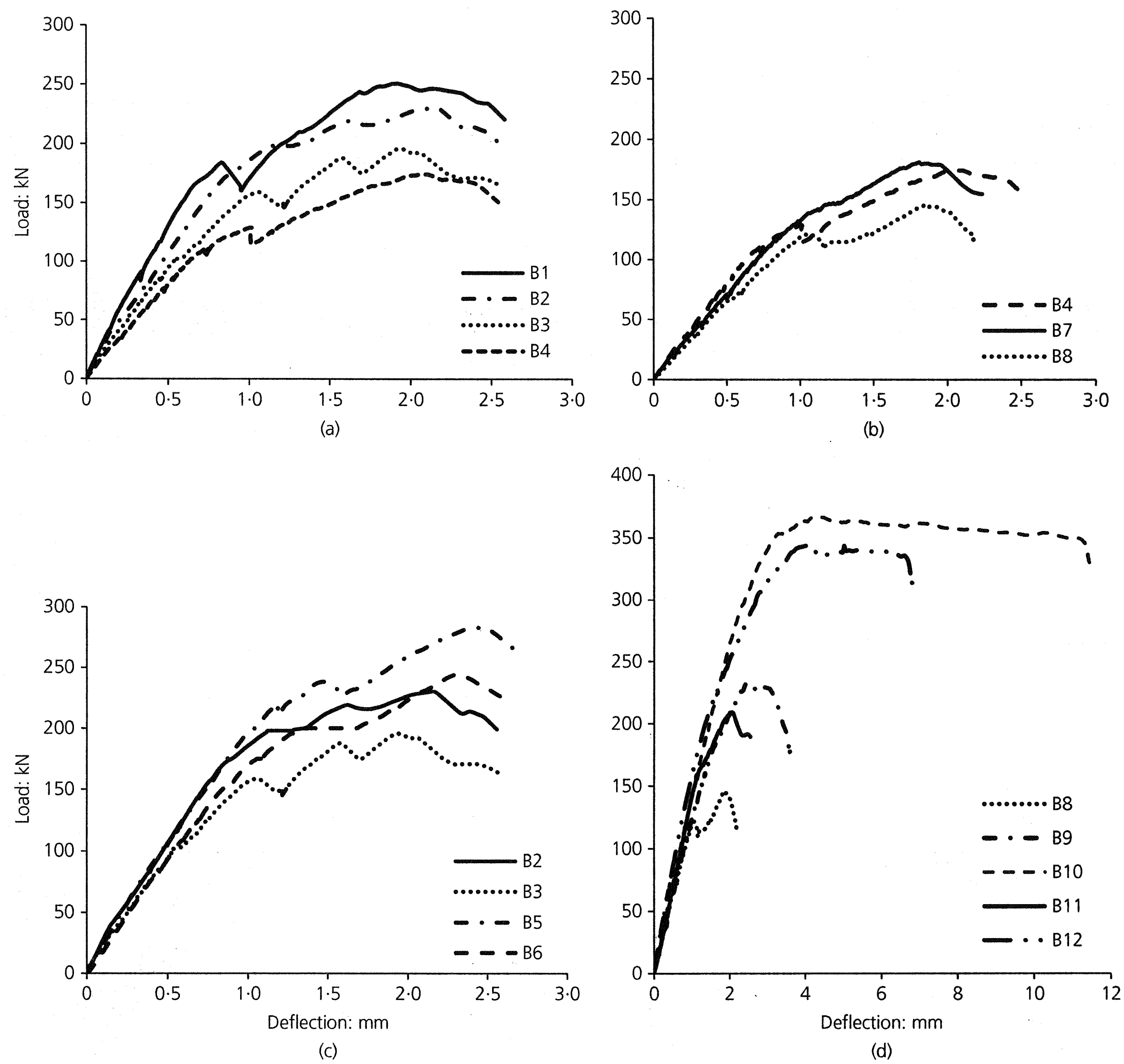


Figure 3. Experimental load–mid-span deflection responses

less brittle behaviour and an obvious improvement in the energy absorption of the tested beams (the area under the load–mid-span deflection curve up to failure load).

## Cracking behaviour

### Effect of CR

As shown in Figure 2 and Table 3, all the SCC/SCRC beams (B1–B4) exhibited a brittle shear failure mode that occurred upon the formation of a major shear diagonal crack starting at the middle height of the beam near one of the supporting points and extending towards the loading zone (compression zone). The failure pattern of beams B2–B4 was characterised by a relatively higher number of cracks and a smaller maximum crack width compared to the beam with no CR (B1). For example, increasing the percentage of CR from 0 to 25% raised the number of cracks at failure from 9 to 11, while the maximum diagonal crack width decreased from 8 mm to 5 mm. Such observations may be related to the fact that the increased deformability of the beams due to inclusion of CR encourages the development of higher levels of cracking in terms of the number of cracks and crack widths. Since the tensile strength of concrete is negatively affected by the inclusion of CR, a larger number of cracks is most likely to develop instead of continuous widening of one localised crack, thus lowering the overall crack widths. Comparing the SCRC and VRC beams (B4 and B7, respectively), it can be seen that the SCRC beam showed larger crack widths and a higher number of cracks at the failure stage, as shown in Table 3 and Figure 2. This finding may be attributed to the higher ultimate deflection exhibited by the SCRC beam compared with its VRC beam counterpart, as illustrated earlier.

### Effect of combining SFs with CR

Figure 2 and Table 3 show that the inclusion of 0·35% SFs (35 or 60 mm) did not change the failure mode of the beams: both SFSCRC beams (B5 and B6) and SFVRC beams (B9 and B11) failed in a shear mode, similar to their SCRC and VRC counterpart beams without SFs (B2 and B3 and B8, respectively). However, the SFs played a significant role in stitching the cracks and developing bridging mechanisms along the crack faces, which in turn limited the crack openings and delayed their propagation. For example, in the SFSCRC beams with 0·35% SFs and 5% and 15% CR (B5 and B6, respectively) the maximum diagonal crack width at failure appeared to decrease by 57·1% and 49·1%, respectively, compared with beams with no SFs (B2 and B3). A similar effect for SFs was confirmed in the SFVRC beams (B9 or B11 compared with B8). Increasing the volume of fibres to 1% further limited the diagonal cracks, in addition to changing the beam failure mode from brittle shear failure to flexural and flexural-secondary shear mode, as shown in B10 and B12, respectively, compared with B8.

## Shear strength

Since the beam mixtures had different 28 d compressive strengths (as shown in Table 2) due to the inclusion of CR with/without SFs, the ultimate shear load ($V_u$) was normalised to account for the effect of different compressive strengths. Knowing that the shear strength is proportional to the square root of the compressive strength of the concrete ($f'_c$), the normalised shear strength ($v_{nz}$) was calculated using

$$v_{nz} = \frac{V_u}{bd\sqrt{f'_c}} \quad (1)$$

### Effect of CR

The normalised shear strengths of all the tested beams are shown in Table 3: the normalised shear strengths of the SCC beams decreased as the percentage of CR increased. Increasing the percentage of CR from 0 to 25% (B1–B4) reduced the normalised shear strength up to 9·1%. Similarly, in the VRC beams (B7 and B8) the normalised shear strength appeared to decline with increases in the percentage of CR. This behaviour may highlight the contribution of CR to decaying the tensile strength of concrete within the region of shear, which in turn allowed diagonal cracks to develop in the beam at relatively lower loads, eventually causing failure. However, the inclusion of CR beneficially contributed to producing semi-lightweight concrete (CSA, 2004); for example, varying the percentage of CR from 15 to 35% achieved mixtures with a density ranging from 2128 to 2014 kg/m$^3$. By comparing the performances of VRC and SCRC (B7 compared with B4), the results show that both VRC and SCRC beams had a comparable normalised shear strength.

### Effect of combining SFs with CR

Table 3 shows that including SFs increased the normalised shear strength. For instance, adding 0·35% SFs to SCRC mixtures improved the normalised shear strength by an average of 23%, as shown by comparing B5 and B6 with B2 and B3, respectively. The reasons for such an increase could be related to (*a*) the contribution of fibres to restricting the widening and propagation of diagonal cracks, thus increasing the aggregate interlock and preserving a bigger uncracked compression zone, and increasing the shear capacity of the beams (Ding *et al.*, 2011) and (*b*) fibres perpendicular to the diagonal cracks may act as aggregate particles with a very elongated shape (Tahenni *et al.*, 2016), which can develop a special type of aggregate–mortar interlock, thus improving the shear transfer capacity. The beneficial impact of SFs on enhancing the normalised shear strength of beams was also confirmed in the VRC beams. The effect of SFs appeared to be more pronounced in beams with high percentages of CR (B9) than those with low CR content (B5 and B6). Adding 0·35% SFs to beams with 35% CR raised the normalised shear strength by 57·5% (B9 compared with B8), and this was more than twice the improvement observed in B5 and B6 with 5% CR and 15% CR, respectively. This may be attributed to the fact that at a higher CR content (35%) the rubber–concrete composite became weaker and more susceptible to the fibres' mechanism in arresting crack growth and improving the aggregate interlock, which then greatly increased the shear capacity of the beams. A similar effect was observed in the STS results: at low CR contents (5% and 15%), adding 0·35% SFs (35 mm) increased the tensile strength by 15·6–17·2%, while with higher CR content (35%) this increase reached 29·1% (Table 2). Increasing the volume of SFs to 1% led to further improvement in the normalised shear strength, reaching up to 242% as much as beams with no SFs (B8). The results also indicate that adding 60 mm long SFs increased the normalised shear strength of beams, but this increase was less than that observed with use of the 35 mm SFs. Using 0·35% and 1% of 60 mm SFs (B11 and B12, respectively) resulted in increases in the normalised shear strength of 42% and 230%, compared with 57·5% and 242% increases in beams with 35 mm SFs (B9 and B10, respectively). These results may be attributed to the fact that, for a given volume of fibres, the number of single fibres increases as the diameter and/or length of fibres decrease, which may raise the probability of single fibres being oriented perpendicularly to the diagonal cracks. This could lead to greater bridging/stitching actions along cracks, which boosts the contribution of fibres to the shear capacity of beams. It is worth noting that combining 15% CR and 0·35% SFs (35 mm) in B6 resulted in a normalised shear strength 12·4% higher than that of the control beam, while a combination of 35% CR and 1% SFs (VRC beams B10 or B12) helped to produce semi-lightweight concrete beams with a normalised shear strength almost twice the value obtained in the beam with no CR (B1).

## Theoretical predictions of shear strength

### SCRC and VRC beams

Four design codes that have gained great approbation worldwide – namely ACI 318 (ACI, 2008), EC2 (BSI, 2005), Aashto LRFD (Aashto, 2007) and CSA A23.3 (CSA, 2004) – were used to predict the ultimate shear capacity of the tested SCC, SCRC and VRC beams. It should be noted that since these code models do not include the effect of SFs in their calculations, only beams without SFs were compared with the predictions from these codes. Details of the equations used are shown in Table 4.

Figure 4(a) shows the ratio of experimental to predicted shear capacity ($V_{exp}/V_{pred}$) for each tested beam. The figure shows that all the code equations highly underestimated the shear strength of SCC, SCRC and VRC beams. Looking closely at the four models, it can be seen that EC2 (BSI, 2005) had the lowest $V_{exp}/V_{pred}$ ratio (i.e. the most accurate predictions). These ratios ranged from 1·10 to 1·39 with a mean and standard deviation (SD) of 1·25 and 0·10, respectively. CSA A23.3 (CSA, 2004) exhibited lower $V_{exp}/V_{pred}$ ratios for B1 and B2 compared with those obtained by the ACI 318 (ACI, 2008) and Aashto LRFD (Aashto, 2007) methods, while the CSA code appeared to be more conservative than ACI 318 and Aashto LRFD for B3 and B4, and B7 and B8. This is attributed to the fact that the predictions of CSA A23.3 for B3, B4, B7 and B8 were subjected to a reduction by a factor of $\lambda = 0{\cdot}85$ as the density of concrete used in those beams fell within the range 1850–2150 kg/m$^3$ (which is classified as a semi-lightweight concrete in CSA A23.3 (CSA, 2004)). Unlike the CSA code, for the case of replacing the total volume of fine aggregate by lightweight sand, ACI 318 (ACI, 2008) and Aashto LRFD (Aashto, 2007) recommend that the reduction factor of $\lambda = 0{\cdot}85$) be applied. Since the rubber partially replaced the fine aggregate, the reduction factor $\lambda$ was linearly interpolated between 0·85 and 1. The results also indicated that increasing the CR content appeared to decrease the $V_{exp}/V_{pred}$ ratios for all the design codes. This is due to the fact that the equations do not take the impact of CR into account, which may indicate a need for further investigations to highlight the rubber–concrete composite's contribution to the shear strength of beams.

### SFSCRC and SFVRC beams

The ultimate shear strengths of SFSCRC and SFVRC beams obtained from the conducted experiments were compared with those predicted by six of the existing models available in the literature; these models include the effect of SFs in their calculations. Details of the equations used are shown in Table 4.

The $V_{exp}/V_{pred}$ ratio for each beam is shown in Figure 4(b). The model developed by Khuntia *et al.* (1999) appears to be the most conservative model of those used here, showing $V_{exp}/V_{pred}$ ratios ranging from 1·58 to 1·98. The models developed by Narayanan and Darwish (1987), Imam *et al.* (1994), and Kwak *et al.* (2002) provided better predictions, with $V_{exp}/V_{pred}$ in the range 1·23–1·57, 1·11–1·30 and 0·95–1·33, respectively. The closest predictions were from the model proposed by Ashour *et al.* (1992), with $V_{exp}/V_{pred}$ in the range 0·96–1·20. Despite the simplicity of the model proposed by Sharma (1986), which does not consider the fibre volume, fibre aspect ratio and/or reinforcement ratio, the model was able to conservatively predict the shear strength of beams with $V_{exp}/V_{pred}$ in the range 1·18–1·59. Examining the predicted values of each model, it can be clearly seen that increasing the percentage of CR resulted in a reduction in $V_{exp}/V_{pred}$ ratio. Further research is thus required to include the effect of CR in these equations in order to safely predict the contribution of CR to the shear strength of fibre–concrete composites.

### Cracking moment

Table 3 lists the cracking moments ($M_{cr}^{exp}$) associated with the first flexural crack. It should be noted that the first flexural crack load was visually observed and then compared/verified with values associated with the change in slope of the load–deflection obtained from the test. The observed cracking moment was also compared with predicted values ($M_{cr}^{pred}$), calculated based on various codes as follows.

According to ACI 318 (ACI, 2008)

2. $$M_{cr}^{pred} = f_r \frac{I_g}{y_t}$$

where $f_r = 0{\cdot}62\lambda\sqrt{f_c'}$ for normal-weight concrete ($\lambda$ is taken as equal to 1 for normal-density concrete and 0·85 for lightweight sand), $y_t$ is the distance from the centroidal axis of the gross section to the extreme tension fibre and $I_g$ is the second moment of area of the gross section (the steel bars are not considered).

As per CSA A23.3 (CSA, 2004)

3. $$M_{cr}^{pred} = f_r \frac{I_g}{y_t}$$

Table 4. Theoretical models of the shear strength for beams with/without SFs and with no stirrups

| Code | Model |
|---|---|
| ACI (2008) | $V_c = \left(0{\cdot}16\,\lambda\sqrt{f'_c} + 17\,\rho\dfrac{d}{a}\right)bd \le 0{\cdot}29\sqrt{f'_c}\,bd$<br>$f'_c$ = cylinder compressive strength (MPa)<br>$\lambda$ = lightweight concrete modification factor (1·0 for normal-weight concrete, 0·85 for sand–lightweight concrete, and 0·75 for all lightweight concrete)<br>$\rho$ = tensile reinforcement ratio<br>$d$ = effective depth of beam (mm)<br>$a$ = shear span (mm)<br>$b$ = width of beam (mm) |
| EC2 | $V_c = [0{\cdot}18\,\eta K(100\rho fc')^{1/3}]bd$<br>$\eta$ = factor to account for lightweight concrete ($\eta = 0{\cdot}4 + 0{\cdot}6\rho/2200$)<br>$K$ = size effect factor ($K = 1 + \sqrt{200/d} \le 2{\cdot}0$) |
| CSA (2004) | $V_c = \beta\lambda\sqrt{f'_c}\,bd_v$<br>$\beta$ = factor accounting for shear resistance of cracked concrete<br>$d_v$ = effective shear depth (the greater of 0·9 times the beam depth or 0·72 times the beam height) |
| Aashto (2007) | $V_c = 0{\cdot}083\beta\,\lambda\sqrt{f'_c}\,bd_v$ |
| **Investigator** | |
| Narayanan and Darwish (1987) | $v_u = \left[2{\cdot}8\dfrac{d}{a}\left(0{\cdot}24\left(\dfrac{f'_c}{20-\sqrt{F}} + 0{\cdot}7 + \sqrt{F}\right) + 80\rho\dfrac{d}{a}\right) + 0{\cdot}41\,\tau F\right]$<br>For $a/d \le 2{\cdot}8$<br>$F$ = fibre factor = $[V_f(l_f/d_f)\,D_f]$<br>$V_f$ = fibre volume<br>$l_f/d_f$ = fibre aspect ratio<br>$D_f$ = the bond factor dependent on the shape of the SFs (0·5 for circular section plain fibre, 0·75 for crimped fibre or hooked fibre, and 1 for indented fibre)<br>$\tau$ = fibre–matrix interfacial bond strength, taken as 4·15 MPa based on recommendations of Swamy *et al.* (1974) |
| Khuntia *et al.* (1999) | $v_u = \left[\left(0{\cdot}167\left(2{\cdot}5\dfrac{d}{a}\right) + 0{\cdot}25\,F\right)\sqrt{f'_c}\right]$<br>For $a/d \le 2{\cdot}5$ (ACI Code Modification)<br>$D_f$ = 2/3 for plain and round, 1·0 for hooked or crimped fibres |
| Ashour *et al.* (1992) | $v_u = \left[\left(0{\cdot}7\sqrt{f'_c} + 7F\right)\dfrac{d}{a} + 17{\cdot}2\,\rho\dfrac{d}{a}\right]$<br>ACI Code Modification |
| Sharma (1986) | $v_u = \left[\dfrac{2}{3}f'_t\left(\dfrac{d}{a}\right)^{0{\cdot}25}\right]$<br>$f'_t$ = splitting tensile strength of concrete (MPa) |
| Imam *et al.* (1994) | $v_u = \left[0{\cdot}6\,\Psi\sqrt[3]{\omega}\left((f'_c)^{0{\cdot}44} + 275\sqrt{\dfrac{\omega}{(a/d)^{0{\cdot}44}}}\right)\right]$<br>where, $\Psi = \dfrac{1+\sqrt{5{\cdot}08/d_a}}{\sqrt{1+d/(25\,d_a)}}$ = size effect<br>$d_a$ is the maximum aggregate size mm; $\omega$ = reinforcement factor = $\rho(1+4F)$; the bond coefficient ($D_f$) for the $F$ factor is taken as 1·0 for hooked fibres = 0·9 for deformed fibres = 0·5 for smooth fibres |
| Kwak *et al.* (2002) | $v_u = \left[3{\cdot}7\left(3{\cdot}4\left(\dfrac{d}{a}\right)\left(\dfrac{f'_c}{20-\sqrt{F}} + 0{\cdot}7 + \sqrt{F}\right)^{2/3}\left(\rho\dfrac{d}{a}\right)^{1/3}\right) + 0{\cdot}8\,(0{\cdot}41\,\tau F)\right]$<br>For $a/d \le 3{\cdot}4$ |

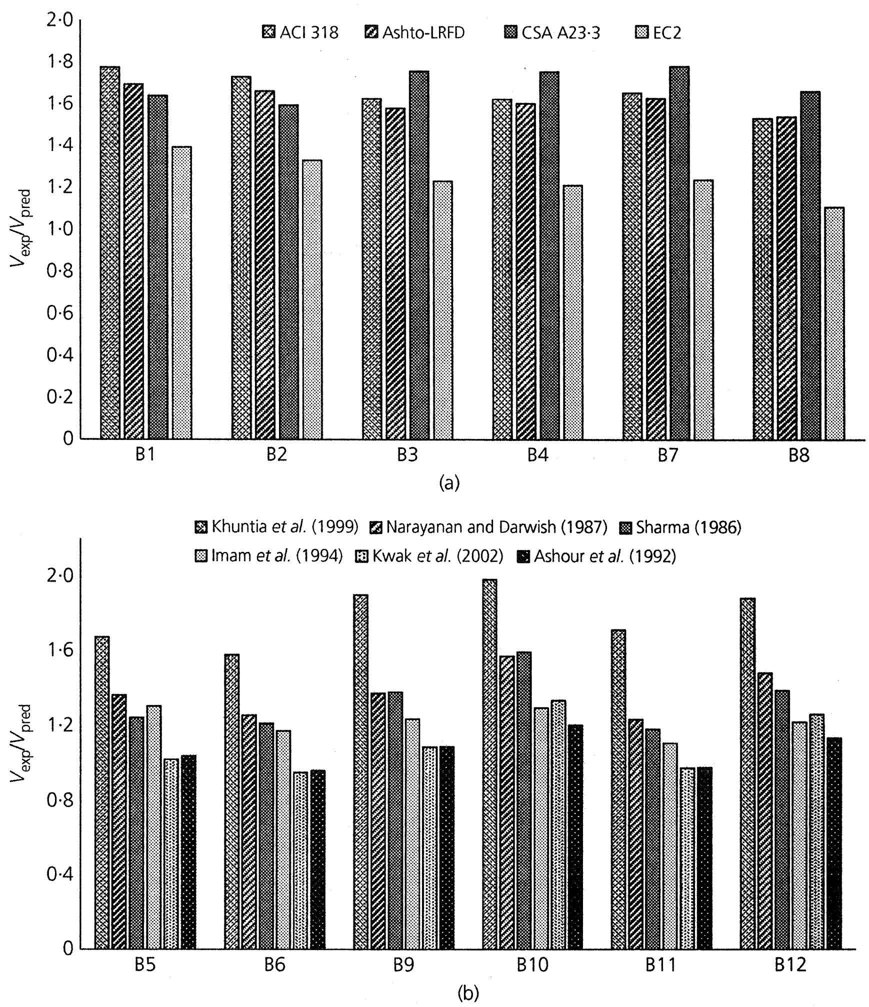


**Figure 4.** Ratio of experimental shear strength to shear strength predicted by (a) code design equations and (b) researchers' models

where $f_r = 0{\cdot}6\lambda\sqrt{f'_c}$ for normal-weight concrete ($\lambda$ is taken as equal to 1 for normal-density concrete and 0·85 for semi-low-density concrete (density in the range 1850–2150 kg/m$^3$).

According to AS 3600 (SA, 1988)

4. $$M_{cr}^{pred} = Zf'_{cf}$$

where $f'_{cf}$ is the characteristic flexural tensile strength of the concrete ($=0{\cdot}6\sqrt{f'_c}$) and $Z$ ($=I/y$) is the section modulus, which is calculated based on the uncracked transformed section, referring to the extreme fibre at which cracking occurs.

EC2 (BSI, 2005) gives

5. $$M_{cr}^{pred} = f_{ctm}\frac{I_u}{(h - x_u)}$$

where $f_{ctm}$ is the mean value of axial tensile strength of concrete ($=0{\cdot}3f_{ck}^{0{\cdot}67}$, $f_{ck}$ is the characteristic compressive cylinder strength of the concrete at 28 d), $I_u$ is the second moment of area of the uncracked transformed section, $x_u$ is the distance from the neutral axis of the section to the extreme top fibre and $h$ is the height of the cross section of the beam.

### SCC, SCRC and VRC beams

As shown in Table 3, the first cracking moment was negatively affected by the inclusion of CR. Varying the CR content from 0 to 25% reduced $M_{cr}^{exp}$ by 40·4% (B1–B4). Such a reduction is attributed to the significant decay in the tensile strength of the concrete when the CR content increased, as shown in the STS test results (Table 2). A similar trend was observed in the SFSCRC and VRC beams (B5–B8), in which $M_{cr}^{exp}$ decreased as the CR content increased.

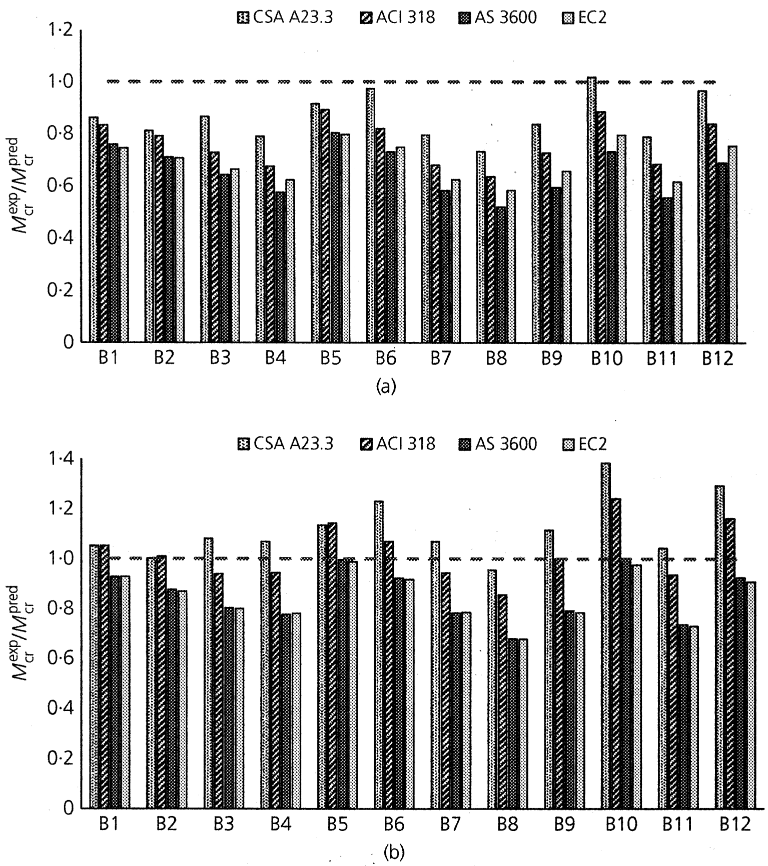


Figure 5. Ratio of the experimental first cracking moment to that predicted by code design equations: (a) based on compressive strength; (b) based on STS

Figure 5 presents the experimental to predicted cracking moment ratio ($M_{cr}^{exp}/M_{cr}^{pred}$) for each tested beam. The predicted cracking moments in this figure were calculated using the code equations based on either a tensile strength derived proportionally from the compressive strength (as proposed by each code design) or using the experimental STS. Figure 5(a) shows $M_{cr}^{exp}/M_{cr}^{pred}$ in which $M_{cr}^{pred}$was calculated based on compressive strength. For the beam with no CR (B1), using the equations proposed by ACI 318, CSA A23.3, AS 3600 and EC2 (Equations 2–5) appeared to overestimate the cracking moment, showing $M_{cr}^{exp}/M_{cr}^{pred}$ ratios ranging from 0·75 to 0·86. Similar observations were reported by other researchers (Fathifazl *et al.*, 2009) when the ACI 318 equation was used to predict the cracking moment of conventional reinforced concrete beams. Figure 5(a) also shows that the inclusion of CR seemed to heighten the error of the codes' predictions. For example, the VRC beam with 35% CR (B8) showed $M_{cr}^{exp}/M_{cr}^{pred}$ in the range 0·52–0·73 (for all code equations). This finding highlights the influence of CR on reducing the tensile strength of concrete.

Using the experimental STS in the code equations to calculate $M_{cr}^{pred}$ (instead of that derived based on compressive strength) generally appeared to exhibit better predictions, as shown in Figure 5(b). For instance, the $M_{cr}^{exp}/M_{cr}^{pred}$ ratios of B1 ranged from 0·93 to 1·05, while B8 (with 35% CR) exhibited $M_{cr}^{exp}/M_{cr}^{pred}$ ratios of 0·68–0·96. The CSA code showed the most conservative predictions, while EC2 and AS 3600 gave higher estimations compared to those of ACI 318 and the CSA model.

### SFSCRC and SFVRC beams

It can be clearly seen from Table 3 that the moment corresponding to the first crack increased with the inclusion of SFs. The SFSCRC beams (B5 and B6) with 0·35% SFs (35 mm) showed an increase in $M_{cr}^{exp}$ (reaching an average of 13·6%) compared with the beams with no SFs (B2 and B3). Similar to the trend of STS and shear capacity results, adding the same amount of SFs to VRC beams with a higher percentage of CR (35%) resulted in a greater improvement in $M_{cr}^{exp}$, which reached 17%, as shown by comparing B9 and B8. Increasing the volume of SFs (35 mm) to 1% (as in B10) raised the $M_{cr}^{exp}$ up to 45·3% higher than the $M_{cr}^{exp}$ of beams with no SFs (B8). These results are attributed to the fibres' mechanism in controlling the development of microcracks and delaying the formation of macrocracks (Ding *et al.*, 2011; Ganesan *et al.*, 2013; Tahenni *et al.*, 2016). Using longer SFs (60 mm) in B11 and B12 also increased the $M_{cr}^{exp}$, but with values 5·9% and 7·2% less than the values exhibited by B9 and B10 with 35 mm SFs, respectively. This may be related to the fact that, at a given fibre volume, using smaller SFs increases the number of fibres that may align in the tensile direction, which effectively helps to delay the formation of macrocracks, as explained earlier.

Examining the predictions of the code equations based on compressive strength shown in Figure 5(a), it can be seen that the inclusion of SFs seemed to decrease the percentage of error in $M_{cr}^{pred}$. For instance, adding 0·35% SFs (35 mm) to SFSCRC beams (B5 and B6) resulted in $M_{cr}^{exp}/M_{cr}^{pred}$ ranging from 0·78 to 0·97, and these values were higher than those shown by B2 and B3 (SFSCRC counterparts). Further increases in the amount of SFs led to more discrepancy between $M_{cr}^{pred}$and $M_{cr}^{exp}$. With 1% 35 mm SFs (B10), the $M_{cr}^{exp}/M_{cr}^{pred}$ ratios ranged from 0·73 to 1·02. Such results are attributed to the fact that the code equations used do not take into account the effect of fibres in the calculation of $M_{cr}^{pred}$, but only consider the 28 d compressive strength, which was unaffected by the inclusion of SFs, resulting in a misleading prediction. Using 60 mm SFs showed a similar effect to the 35 mm SFs. In the second method of calculating the $M_{cr}^{pred}$ based on STS, it was found that using the STS values of SFSCRC or SFVRC in the code equations highly overestimated the cracking moment. It should be noted that, although the tensile strength associated with the first cracking load may have been improved by the inclusion of SFs (as shown by the improved $M_{cr}^{exp}$ of B9–B12 compared with B8), it might not be reliable to use ultimate STS test results to predict the cracking moment. This is because, as observed in the STS tests, after the tested cylinders experienced first cracking, the fibres' bridging mechanism allowed the samples to sustain more loading until pullout of the fibres. Since it is not easy to detect the contribution of fibres to increasing the tensile strength of the first crack in STS tests, it may be possible to use the STS of the counterpart SFSCRC and SFVRC mixtures with no SFs in order to predict the cracking moment. For example, as seen from Figure 5(b), using the STS values of B2 and B3 mixtures to calculate the $M_{cr}^{pred}$ of B5 and B6 showed acceptable estimations, in which the $M_{cr}^{exp}/M_{cr}^{pred}$ ratio ranged from 0·92 to 1·23. Similar results were observed when the STS of mixture B8 was used to predict the $M_{cr}^{pred}$ of the SFVRC beams (B9–B12). However, as explained earlier, similar to the results on SCRC and VRC, EC2 and AS 3600 exhibited lower $M_{cr}^{exp}/M_{cr}^{pred}$ ratios than those of ACI 318 and CSA A23.3.

## Conclusions

The following conclusions can be drawn from the results of this study.

(*a*) Using lightweight crumb rubber (CR) aggregate with low stiffness contributed to increasing the deformability of the tested beams at a given load and also reduced their self-weight. However, increasing the percentage of CR (0 to 25%) in self-consolidating rubberised concrete (SCRC) beams decreased their normalised shear strength by 9·1%. This reduction seemed to be higher for larger percentages of CR (more than 25%).

(*b*) The addition of 0·35% steel fibres (SFs) (35 mm length) to SCRC beams with up to 15% CR increased their normalised shear strength by 23% (on average), while this increase reached 57·5% in vibrated rubberised concrete (VRC) beams with a higher percentage of CR (35%). Increasing the volume of SFs to 1% (in VRC beams with 35% CR) showed a 242% improvement in the normalised shear strength. Also, using longer SFs (60 mm) (in VRC beams with 35% CR) increased the normalised shear strength, but to less than that obtained by the short SFs (35 mm).

(*c*) Beams with up to 35% CR showed a failure mode similar to the beam with no CR (shear failure), but which was characterised by a larger number of cracks and narrower crack widths. The inclusion of 0·35% SFs (35 or 60 mm) and up to 35% CR in steel-fibre-reinforced SCRC and VRC (SFSCRC and SFVRC) beams continued to reduce the crack widths but with no change in the failure mode. Increasing the SF volume to 1% further narrowed the crack widths and changed the failure mode from shear to shear-flexure failure (in beams with 60 mm long fibres) or to flexure failure (in beams with 35 mm long fibres).

(*d*) The investigated design codes (ACI 318 (ACI, 2008), EC2 (BSI, 2005), Aashto LRFD (Aashto, 2007) and CSA A23.3 (CSA, 2004)) were found to be conservative in predicting the ultimate shear strength of beams without SFs (SCC, SCRC and VRC). EC2 showed the most reasonable predictions for the shear strength compared with the other design codes. Comparing the CSA, ACI and Aashto-LRFD results, the CSA code gives a better prediction for normal-weight concrete. However, for semi-lightweight concrete, the values predicted by the Aashto-LRFD appeared to be closer to the values obtained in the experiments.

(*e*) In the shear strength prediction of beams with SFs (SFSCRC and SFVRC), the equation developed by Khuntia *et al.* (1999) showed the highest $V_{exp}/V_{pred}$ values of all the equations used. The accuracy of the estimation was improved using the models proposed by Sharma (1986), Narayanan and Darwish (1987) and Imam *et al.* (1994). On the other hand, although the most reasonable prediction was shown by the equations of Ashour *et al.* (1992) and Kwak *et al.* (2002), these models slightly overestimated some strengths with a percentage of less than 5%, which may lead to unsatisfactory design.

(*f*) Although most of the code equations and shear design models satisfactorily predicted the shear strength of beams containing CR with/without SFs, increasing the CR content negatively affected their conservatism. This finding may indicate that further investigations are required to take the influence of CR into account in the prediction of the shear capacity of beams with/without SFs.

(*g*) Use of the ACI 318, CSA, AS 3600 (SA, 1988) and EC2 equations (based on tensile strength derived from compressive strength) obviously overestimated the first cracking moment values compared with those obtained from experiments, even for the beam with no CR. Increasing the CR content appeared to further reduce the experimental first cracking moment compared with the predicted values in all the tested code-based equations. On the other hand, using the investigated code equations based on the experimental splitting tensile strength (STS) (instead of the value derived from compressive strength) generally gave better predictions, especially when the CSA and ACI 318 equations were used. Similarly, estimating the cracking moment of SFSCRC and SFVRC beams using the STS of their counterpart mixtures with no SFs provided more reliable and satisfactory predictions.

## Acknowledgements

The authors would like to acknowledge the Research & Development Corporation of Newfoundland and Labrador (RDC) for sponsoring this work as part of a larger research project.

### REFERENCES

Aashto (Association of State Highway and Transportation Officials) LRFD (2007) *Bridge Design Specifications and Commentary, SI Units.* Aashto, Washington, DC, USA.

Abadel A, Abbas H, Almusallam T, Al-Salloum Y and Siddiqui N (2015) Mechanical properties of hybrid fibre-reinforced concrete – analytical modelling and experimental behaviour. *Magazine of Concrete Research* **68(16)**: 1–21, http://dx.doi.org/10.1680/jmacr.15.00276/

ACI (American Concrete Institute) (2008) ACI 318R-08: Building code requirements for structural concrete and commentary. ACI, Farmington Hills, MI, USA.

Altun F and Aktas B (2013) Investigation of reinforced concrete beams behavior of steel fibre added lightweight concrete. *Construction and Building Materials* **38**: 575–581.

Ashour SA, Hasanain GS and Wafa FF (1992) Shear behavior of high-strength fiber-reinforced concrete beams. *ACI Structural Journal* **89(2)**: 176–184.

ASTM (2011a) ASTM C39: Standard test method for compressive strength of cylindrical concrete specimens. ASTM International, West Conshohocken, PA, USA.

ASTM (2011b) C496: Standard test method for splitting tensile strength of cylindrical concrete specimens. ASTM International, West Conshohocken, PA, USA.

ASTM (2012a) C618: Standard specification for coal fly ash and raw or calcined natural pozzolan for use in concrete. ASTM International, West Conshohocken, PA, USA.

ASTM (2012b) C150/C150M: Standard specification for Portland cement. ASTM International, West Conshohocken, PA, USA.

ASTM (2013) C494/C494M: Standard specification for chemical admixtures for concrete. ASTM International, West Conshohocken, PA, USA.

ASTM (2014) C231/C231M: Standard test method for air content of freshly mixed concrete by the pressure method. ASTM International, West Conshohocken, PA, USA.

ASTM (2015) C143/C143M: Standard test method for slump of hydraulic-cement concrete. ASTM International, West Conshohocken, PA, USA.

Baston G, Jenkins E and Spatney R (1972) Steel fibers as shear reinforcement in beams. *ACI Journal Proceedings* **69(10)**: 640–644.

Bazant Z and Sun H (1987) Size effect in diagonal shear failure: influence of aggregate size and stirrups. *ACI Materials Journal Proceedings* **84(4)**: 259–272.

BSI (2005) BS EN 1992-1-1: Eurocode 2 – Design of Concrete Structures – Part 1-1: General rules and rules for buildings. BSI, London, UK.

CSA (Canadian Standards Association) (2004) CSA A23.3-04: Design of concrete structures. CSA, Rexdale, ON, Canada.

Ding Y, Liu S, Zhang Y and Thomas A (2008) The investigation of workability of fibre cocktail reinforced self-compacting high performance concrete. *Construction and Building Materials* **22(7)**: 1462–1470.

Ding Y, You Z and Jalali S (2011) The composite effect of steel fibres and stirrups on the shear behaviour of beams using self-consolidating concrete. *Engineering Structures* **33(1)**: 107–117.

Ding Y, Zhang F, Torgal F and Zhang Y (2012) Shear behaviour of steel fibre reinforced self-consolidating concrete beams based on the modified compression field theory. *Composite Structures* **94(8)**: 2440–2449.

Efnarc (European Federation for Specialist Construction Chemicals and Concrete Systems) (2005) *The European Guidelines for Self-Compacting Concrete: Specification, Production and Use.* Efnarc, Norfolk, UK.

Fathifazl G, Razaqpur AG, Isgor OB *et al.* (2009) Flexural performance of steel-reinforced recycled concrete beams. *ACI Structural Journal* **106(6)**: 858–867.

Ganesan N, Bharati RJ and Shashikala AP (2013) Behavior of self-consolidating rubberized concrete beam–column joints. *ACI Materials Journal* **110(6)**: 697–704.

Ganesan N, Indira PV and Santhakumar A (2014) Influence of steel fibres on tension stiffening and cracking of reinforced geopolymer concrete. *Magazine of Concrete Research* **66(6)**: 268–276, http://dx.doi.org/10.1680/macr.13.00273.

Güneyisi E (2010) Fresh properties of self-compacting rubberized concrete incorporated with fly ash. *Materials and Structures* **43(8)**: 1037–1048.

Imam M, Vandewalle L and Mortelmans F (1994) *Shear Capacity of Steel Fiber High Strength Concrete Beams.* American Concrete Institute, Farmington Hills, MI, USA, ACI SP 149, pp. 227–242.

Iqbal S, Ali A, Holschemacher K and Thomas AB (2015) Mechanical properties of steel fibre reinforced high strength lightweight self-compacting concrete (SHLSCC). *Construction and Building Materials* **98**: 325–333.

Ismail MK and Hassan AAA (2015a) Performance of full-scale self-consolidating rubberized concrete beams in flexure. *ACI Materials Journal* **113(2)**: 207–218.

Ismail MK and Hassan AAA (2015b) Influence of mixture composition and type of cementitious materials on enhancing the fresh properties and stability of self-consolidating rubberized concrete. *Journal of Materials in Civil Engineering.*

Ismail MK and Hassan AAA (2016a) Impact resistance and mechanical properties of self-consolidating rubberized concrete reinforced with steel fibers. *Journal of Materials in Civil Engineering* **28(1)**, http://dx.doi.org/10.1061/(ASCE)MT.1943-5533.0001338.

Ismail MK and Hassan AAA (2016b) Use of metakaolin on enhancing the mechanical properties of self-consolidating concrete containing high percentages of crumb rubber. *Journal of Cleaner Production* **125**: 282–295.

Khaloo A, Raisi EM, Hosseini P and Tahsiri H (2014) Mechanical performance of self-compacting concrete reinforced with steel fibers. *Construction and Building Materials* **51**: 179–186.

Khuntia M, Stojadinovic B and Goel S (1999) Shear strength of normal and high-strength fiber-reinforced concrete beams without stirrups. *ACI Structural Journal* **96(2)**: 282–289.

Kwak YK, Eberhard M, Kim WS and Kim J (2002) Shear strength of steel fibre-reinforced concrete beams without stirrups. *ACI Structural Journal* **99(4)**: 530–538.

Lee JH, Yoo DY and Yoon YS (2016) Mechanical behaviour of concrete with amorphous metallic and steel fibres. *Magazine of Concrete Research* **68(24)**: 1253–1264, http://dx.doi.org/10.1680/jmacr.15.00493.

Najim KB and Hall MR (2010) A review of the fresh/hardened properties and applications for plain-(PRC) and self-compacting rubberised concrete (SCRC). *Construction and Building Materials* **24(11)**: 2043–2051.

Najim KB and Hall MR (2012) Mechanical and dynamic properties of self-compacting crumb rubber modified concrete. *Construction and Building Materials* **27(1)**: 521–530.

Najim KB and Hall MR (2014) Structural behaviour and durability of steel-reinforced structural plain/self-compacting rubberised concrete (PRC/SCRC). *Construction and Building Materials* **73**: 490–497.

Narayanan R and Darwish IYS (1987) Use of steel fibres as shear reinforcement. *ACI Structural Journal* **84(3)**: 216–227.

Olivito RS and Zuccarello FA (2010) An experimental study on the tensile strength of steel fibre reinforced concrete. *Composites Part B: Engineering* **41(3)**: 246–255.

SA (Standards Australia) (1988) AS 3600: Concrete structures. SA, Sydney, Australia.

Sadek DM and El-Attar MM (2014) Structural behaviour of rubberized masonry walls. *Journal of Cleaner Production* **89**: 174–186.

Sharma AK (1986) Shear strength of steel fiber reinforced concrete beams. *ACI Journal Proceedings* **83(4)**: 624–628.

Swamy RN, Mangat PS and Rao CVSK (1974) The mechanics of fiber reinforcement of cement matrices. *Fiber Reinforced Concrete.* American Concrete Institute, Farmington Hills, MI, USA, ACI SP 44, pp. 1–28.

Tahenni T, Chemrouk M and Lecompte T (2016) Effect of steel fibres on the shear behavior of high strength concrete beams. *Construction and Building Materials* **105**: 14–28.

Taylor HPJ (1974) *The Fundamental Behavior of Reinforced Concrete Beams in Bending and Shear.* American Concrete Institute, Farmington Hills, MI, USA, ACI SP 42, pp. 43–77.

Topçu IB and Bilir T (2009) Experimental investigation of some fresh and hardened properties of rubberized self-compacting concrete. *Materials and Design* **30(8)**: 3056–3065.

Youssf O, El-Gawady MA and Mills JE (2015) Experimental investigation of crumb rubber concrete columns under seismic loading. *Structures* **3**: 13–27.

Zheng L, Sharon HX and Yuan Y (2008) Experimental investigation on dynamic properties of rubberized concrete. *Construction and Building Materials* **22(5)**: 939–947.

Zsutty T (1971) Shear strength prediction for separate categories of simple beam tests. *ACI Journal Proceedings* **68(2)**: 138–143.

## How can you contribute?

To discuss this paper, please submit up to 500 words to the editor at journals@ice.org.uk. Your contribution will be forwarded to the author(s) for a reply and, if considered appropriate by the editorial board, it will be published as a discussion in a future issue of the journal.